J. Fluid Mech. (1991), *vol.* 224, *pp.* 485–505
Printed in Great Britain

Studies of the Eulerian–Lagrangian transformation in two-dimensional random flows

By J. P. LYNOV, A. H. NIELSEN, H. L. PÉCSELI AND J. JUUL RASMUSSEN

Association EURATOM-Risø National Laboratory, Optics and Fluid Dynamics Department, Risø, DK-4000 Roskilde, Denmark

(Received 2 March 1990)

Two-dimensional, incompressible flows are discussed by a generalization of the line-vortex model. A large number of structures are randomly distributed initially. Each individual structure is convected by the superposed flow field of all the others. The statistical properties of the resulting space–time varying random flow are studied. Analytical expressions for both Eulerian and Lagrangian correlation functions are obtained for the limit where the density of structures is large. The analytical results compare favourably with numerical simulations. The study serves as a special test on proposed relations between Eulerian and Lagrangian averages which can be generally valid, i.e. also for three-dimensional, turbulent flows.

1. Introduction

The dynamics of two-dimensional flows present a number of interesting problems which can be tested numerically even with modest computer resources. In the present study we take advantage of the ease with which two-dimensional flows can be simulated numerically, using a generalized version of Onsager's (1949) interacting line-vortex model. In particular some specific theoretical results of Wandel & Kofoed-Hansen (1962) and Pécseli & Mikkelsen (1985) for the relations between Eulerian and Lagrangian averages can then be tested with good accuracy under well-defined conditions in two-dimensions, although the results in their most general form are applicable to fully three-dimensional conditions as well.

Originally Wandel & Kofoed-Hansen (1962) set out to provide a theoretical basis for the hypothesis of Hay & Pasquill (1960) which gives a phenomenological relation between the power spectra $P_{\mathrm{L}}(\omega)$ and $P_{\mathrm{E}}(\omega)$ obtained by Lagrangian and Eulerian sampling, respectively, of the turbulent velocity fluctuations. They suggested a simple scaling as

$$P_{\mathrm{L}}(\omega) \approx \beta P_{\mathrm{E}}(\beta\omega), \tag{1}$$

where the constant β was determined empirically to be in the range $2 < \beta < 4$. In terms of the correlation functions the relation (1) becomes

$$R_{\mathrm{L}}(\beta\tau) \approx R_{\mathrm{E}}(\tau). \tag{2}$$

Rather than approaching the problem by the Navier–Stokes equation, Wandel & Kofoed-Hansen (1962) considered an autonomous system which for certain parameters have turbulence-like features. They thus assumed a flow field $\boldsymbol{v}(\boldsymbol{r}, t)$ obtained by superposition of many structures, i.e.

$$\boldsymbol{v}(\boldsymbol{r}, t) = \sum_{l}^{N} \boldsymbol{u}_l(\boldsymbol{r} - \boldsymbol{r}_l). \tag{3}$$

An autonomous model is obtained by requiring that individual structures, or eddies, are convected by the flow generated by all the others, i.e.

$$\frac{\mathrm{d}\boldsymbol{r}_l(t)}{\mathrm{d}t} = \sum_{k\neq l}^{N} \boldsymbol{u}_k(\boldsymbol{r}_l - \boldsymbol{r}_k). \tag{4}$$

By studying systems described in (3)–(4) with some simplifying assumptions Wandel & Kofoed-Hansen (1962) suggested a value for β in (1)–(2) which depended explicitly on the r.m.s. value of the velocity fluctuations, and the mean flow velocity, $\langle v\rangle$, as $\beta = (\frac{1}{4}\pi^{\frac{1}{2}})(\langle v\rangle/u')$, where $u'^2 \equiv \frac{1}{3}\langle u^2\rangle$ in three dimensions in the limit where $\langle v\rangle \gg u'$. This result has been recognized in the literature, see e.g. Panofsky & Dutton (1984). The analysis is, however, much more general and contains a fundamental result in terms of explicit relations between Eulerian and Lagrangian velocity correlations. It is our aim to study and analyse these relations. For this purpose a numerical code was developed in which a system containing a large number of structures and evolving in accordance with (3)–(4) is simulated. Although the formulation of these equations allows, in principle, a full three-dimensional modelling, our calculations are, as mentioned, restricted to two dimensions. This analysis is relevant also for other physical systems, such as certain types of low-frequency plasma turbulence, which may be quite well described by a two-dimensional model (Joyce & Montgomery 1973; Seyler *et al.* 1975; Huld *et al.* 1988; Knorr & Pécseli 1989).

In two dimensions (3) and (4) are rewritten conveniently as

$$\boldsymbol{v}(\boldsymbol{r},t) = \nabla\Phi \times \hat{\boldsymbol{e}} = \sum_{l}^{N} \nabla\phi_l(\boldsymbol{r} - \boldsymbol{r}_l(t)) \times \hat{\boldsymbol{e}}, \tag{5}$$

and

$$\frac{\mathrm{d}\boldsymbol{r}_l(t)}{\mathrm{d}t} = \sum_{k\neq l}^{N} \nabla\phi_k(\boldsymbol{r}_l - \boldsymbol{r}_k) \times \hat{\boldsymbol{e}}, \tag{6}$$

where introduction of the stream function Φ ensures that the flow is incompressible, $\nabla \cdot \boldsymbol{v}(\boldsymbol{r},t) = 0$. The unit vector $\hat{\boldsymbol{e}}$ is perpendicular to the plane confining the system. The vorticity associated with the flow is $\omega = -\nabla^2\Phi = -\sum_l^N \nabla^2\phi_l(\boldsymbol{r} - \boldsymbol{r}_l)$. The number of structures in the system, N, is varying randomly over the ensemble of realizations according to a Poisson distribution. Elements of this model can be found also in the paper by Chorin (1973). In particular, Onsager's (1949) line-vortex model is a special case of (5)–(6) with the choice $\phi_k(\boldsymbol{r}) = A_k \ln(|\boldsymbol{r}|)$. It is readily demonstrated that the dynamical system of structures described by (5)–(6) can be put in a Hamiltonian form for $\phi_k = A_k F(|\boldsymbol{r}|)$ where $F(r)$ is an arbitrary function and A_k is a constant. With

$$H = \sum_{l>k} A_l A_k F(|\boldsymbol{r}_l - \boldsymbol{r}_k|), \tag{7}$$

the generalized coordinates are related to the (x,y)-coordinates in configuration space by

$$(q_l, p_l) = |A_l|^{\frac{1}{2}}(x_l, y_l \operatorname{sign}(A_l)), \tag{8}$$

i.e. $\mathrm{d}p_l/\mathrm{d}t = -\partial H/\partial q_l$ and $\mathrm{d}q_l/\mathrm{d}t = \partial H/\partial p_l$. The notation $l > k$ in the summation in (7) indicates that each pair of structures is counted only once. Since H is not an explicit function of time, it is a constant of motion for an isolated system. The Hamiltonian (7) accounts for an effective potential energy of the interacting structures, as evident by considering the particular line-vortex model. The system does not possess any kinetic energy in the usual sense (Joyce & Montgomery 1973).

The Hamiltonian (7) applies in the absence of boundaries. The presence of periodic boundary conditions requires the introduction of a modified potential for F (Ewald 1921).

It is clear from the construction that the individual structures, specified by ϕ_l in (5) and (6) or by F in (7), are not distorted by the flow. The lengthscales of the structures are thus imposed *a priori* and will characterize the flow at all times. However, any macroscopic arrangement of many individual structures will be distorted and sheared by the flow. The velocity field (5) will therefore have properties in common with flows described by two-dimensional Euler equations although the two equations governing the time evolutions of the flows are different. Evidently any flow described by (5) with smooth initial condition will remain smooth for any later time, i.e. no discontinuities will develop. Also these properties are consistent with those characterizing flows described by the Euler equation in two dimensions (Sulem & Sulem 1983; Sulem, Sulem & Frisch 1983).

From (8) it is readily concluded that phase space is finite for a confined system. Onsager (1949) pointed out that for such systems the temperature may take on negative values. In such cases the system is expected to be characterized by an ordering of structures, (or eddies), appearing as a clustering of structures having the same sign of the amplitude, A_k, as discussed also by Joyce & Montgomery (1973) and Montgomery & Joyce (1974). This clustering can be argued in a particularly simple way for the line-vortex model: for a finite physical domain the only way to increase the energy content of the system indefinitely is to place like-signed vortices close to each other, resulting in macroscopically organized structures. (Recall that $T = \mathrm{d}Q/\mathrm{d}S$, where T is the temperature, Q is the energy while the entropy S can be taken as a measure of the disorder of the system. The inverse temperature is a measure of the change of disorder of a system per unit change in energy. The actual value of the system energy where the temperature changes sign is subject to some controversy.) On the other hand, the positive temperature states, which will be studied in the present work, are expected to be characterized by complete randomness, i.e. a structure can at any time be found with equal probability in any area element of phase space, irrespective of the position of the other structures. Explicit use of this feature will be made in the subsequent analysis. The negative temperature states were avoided by choosing initial states with low values of the Hamiltonian (Joyce & Montgomery 1973).

Our analysis was restricted to two spatial dimensions in order to reduce the demands on computer resources. Even this restricted study is, however, of physical relevance in connection with certain types of low-frequency electrostatic turbulence in strongly magnetized plasmas (Huld *et al.* 1988). In these cases magnetic field lines can be considered equi-potential, and a two-dimensional description (Joyce & Montgomery 1973) in the plane perpendicular to the magnetic field, $\boldsymbol{B}$, is appropriate. Line charges are here the analogues of the vortices. They give rise to a spatially varying electrostatic field, $\boldsymbol{E}$, and the slow movement of the guiding centres is given by the $\boldsymbol{E}\times\boldsymbol{B}/B^2$-velocity. It is interesting to note that in this problem the electrostatic potential, which is a readily measurable quantity, takes the role of the stream function. Turbulent diffusion of charged particles across magnetic field lines is a particularly pertinent problem for present day fusion research.

The paper is organized as follows: in §2 the results and arguments of Wandel & Kofoed-Hansen (1962) are summarized, with particular attention to the two-dimensional formulation of their analysis as discussed by Pécseli & Mikkelsen (1985). An alternative simple derivation of these results is presented, which gives an insight

into the assumptions underlying the analysis. Our numerical results are presented in §3 and compared with the expressions obtained in §2. Finally, §4 contains our conclusions, where the implications of the results for analysis of turbulent diffusion are discussed.

2. Analytical results

In the first part of this section we summarize the main results of Wandel & Kofoed-Hansen (1962) and given in more detail by Kofoed-Hansen & Wandel (1967). Their study is concerned with model systems described by (3)–(4), which are analysed in certain limits described by parameters characterizing the system. One of the parameters is the normalized density of structures μ, while an other one ϵ is a characteristic of the wavenumber spectrum of the turbulence, expressed in terms of wavenumbers raised to some power, and averaged over the entire spectrum. The most important of these two parameters is μ, which for a given area of the system is a measure of the average number of structures, i.e. the number of degrees of freedom in the system. In this sense μ can be interpreted as being proportional to an effective Reynolds number.

2.1. *Summary of basic analytical results*

In the present work we study in particular the correlation functions for the velocity fluctuations. The velocity field is sampled either along a trajectory $\boldsymbol{r} = \boldsymbol{r}(t)$, where $\boldsymbol{r} = \boldsymbol{v}_0 t$ with $\boldsymbol{v}_0 =$ constant, which corresponds to Eulerian sampling (in particular we may have $v_0 = 0$), or along $\boldsymbol{r}(t) = \int_0^t \boldsymbol{v}(\boldsymbol{r}(\tau), \tau)\,\mathrm{d}\tau$ with $\boldsymbol{v}$ given by (5), which corresponds to the Lagrangian sampling with velocity $\boldsymbol{u}(t) = \boldsymbol{v}(\boldsymbol{r}(t), t)$. The normalized Lagrangian correlation functions can be written as a series expansion (Hinze 1975)

$$R_{\mathrm{L}}(\tau) \equiv \langle \boldsymbol{u}(t) \cdot \boldsymbol{u}(t+\tau) \rangle = 1 + \sum_{n=1}^{\infty} \tau^{2n} \frac{(-1)^n}{(2n)!} \frac{\langle (\mathrm{d}_t^n \boldsymbol{u})^2 \rangle}{\langle u^2 \rangle}, \tag{9}$$

where angle brackets denote ensemble averages. Time stationarity is assumed, i.e. R_{L} is a function of time separations only and does not depend explicitly on both t and τ. The symmetry property $R_{\mathrm{L}}(\tau) = R_{\mathrm{L}}(-\tau)$ was explicitly used. It is assumed that each of the terms in (9) is finite and that $R_{\mathrm{L}}(\tau \to \infty) \to 0$. Situations may formally exist where the series (9) diverges or the series expansion is not feasible. These cases are not considered here. As the first step the eigenmotion of the eddies is ignored, i.e. $\boldsymbol{r}_l =$ constant in (3)–(4). This limit corresponds to analysing the transport properties of a frozen flow where the velocity varies with position but not with time. A basic result of Wandel & Kofoed-Hansen (1962) admits, in the limit $\mu \to \infty$ and $\epsilon \to 0$, the approximation

$$\begin{aligned} \langle (\mathrm{d}_t^n \boldsymbol{u})^2 \rangle &= \langle [(\boldsymbol{u} \cdot \boldsymbol{\nabla})^n \boldsymbol{u}]^2 \rangle \approx \langle (|\boldsymbol{u}|^n (\boldsymbol{e} \cdot \boldsymbol{\nabla})^n \boldsymbol{u})^2 \rangle \\ &\approx \langle u^{2n} \rangle \cdot \langle [(\boldsymbol{e} \cdot \boldsymbol{\nabla})^n \boldsymbol{u}]^2 \rangle, \end{aligned} \tag{10}$$

for homogeneous, isotropic turbulence, where $\boldsymbol{e}$ is an arbitrary unit vector in the plane confining $\boldsymbol{u}$. Introducing the power-spectrum $\mathscr{E}(k)$ for the velocity fluctuations we use the definition for $\langle k^{2n} \rangle = \int_0^\infty k^{2n} \mathscr{E}(k)\,\mathrm{d}k$. Equation (10) can then be rewritten as

$$\frac{\langle (\mathrm{d}_t^n \boldsymbol{u})^2 \rangle}{\langle u^2 \rangle} \approx \langle u^{2n} \rangle \langle k^{2n} \rangle. \tag{11}$$

In the limit of large μ and randomly distributed structures, the components of $\boldsymbol{u}$ are normally distributed by the central limit theorem, and $\langle u^{2n} \rangle$ is readily calculated for

all n. In particular $\int_0^\infty \mathscr{E}(k)\,\mathrm{d}k = 1$. It was subsequently demonstrated that the random motion of the individual structures could be accounted for simply by replacing $\boldsymbol{u}$ in $\langle u^{2n}\rangle$ by the average velocity difference between individual structures and the test particle. Since structures are transported like particles according to (6), their velocity distribution can be taken to be the same Gaussian as that of the test particle. Since many structures contribute to the local particle velocity, the respective velocity of an individual structure and a particle may be considered statistically independent to a good approximation. With these approximations applied to the two-dimensional geometry, Pécseli & Mikkelsen (1985) obtained

$$R_{\mathrm{L}}(\tau) = \int_0^\infty \mathscr{E}(k)\, W(k\tau\langle u^2\rangle^{\frac{1}{2}})\,\mathrm{d}k, \tag{12}$$

where

$$W(\zeta) = 1 - \zeta \exp(-\tfrac{1}{2}\zeta^2) \int_0^\zeta \exp(\tfrac{1}{2}\gamma^2)\,\mathrm{d}\gamma. \tag{13}$$

The function $W(\zeta)$ is closely related to the Dawson integral. The differences in $R_{\mathrm{L}}(\tau)$ for two and three dimensions originate in the calculations of $\langle u^{2n}\rangle$ in (10) with a Gaussian distribution of the two, respectively three, velocity components.

The Eulerian velocity correlation function $R_{\mathrm{E}}(\tau)$ can be calculated similarly. Considering first the frozen flow, the velocity field is sampled along a trajectory $\boldsymbol{r} = \boldsymbol{v}_0 t$ with constant probing velocity $\boldsymbol{v}_0$, i.e. $\boldsymbol{v}(t) = \boldsymbol{v}(r = \boldsymbol{v}_0 t)$ for this case. An expression corresponding to (9) is of course valid also for $R_{\mathrm{E}}(\tau)$, but (10) is now replaced by

$$\begin{aligned}\langle(\mathrm{d}_t^n \boldsymbol{v})^2\rangle &= \langle[(\boldsymbol{v}_0\cdot\boldsymbol{\nabla})^n \boldsymbol{v}]^2\rangle = \langle(|\boldsymbol{v}_0|^n (\boldsymbol{e}\cdot\boldsymbol{\nabla})^n \boldsymbol{v})^2\rangle \\ &= v_0^{2n}\langle[(\boldsymbol{e}\cdot\boldsymbol{\nabla})^n \boldsymbol{v}]^2\rangle,\end{aligned} \tag{14}$$

or

$$\frac{\langle(\mathrm{d}_t^n \boldsymbol{v})^2\rangle}{\langle v^2\rangle} = v_0^{2n}\langle k^{2n}\rangle, \tag{15}$$

which is now an exact relation. The random motion of eddies was accounted for by replacing v_0 in (15) by the velocity difference between the probe and the local flow velocity, i.e. writing

$$\frac{\langle(\mathrm{d}_t^n \boldsymbol{v})^2\rangle}{\langle v^2\rangle} \approx \langle|\boldsymbol{v}_0 - \boldsymbol{v}|^{2n}\rangle\,\langle k^{2n}\rangle, \tag{16}$$

where $\boldsymbol{v}$ on the right-hand side is assumed to have components with a Gaussian distribution, by the same arguments as before. The explicit result is given by Pécseli & Mikkelsen (1986) as

$$R_{\mathrm{E}}(\tau) = \int_0^\infty \mathscr{E}(k)\, S\left(k\tau u', \frac{v_0}{u'}\right)\mathrm{d}k, \tag{17}$$

where $u'^2 \equiv \frac{1}{2}\langle v^2\rangle$ and

$$S(x, y) = \exp(-\tfrac{1}{2}y^2) \int_0^\infty \cos(x\gamma)\exp(-\tfrac{1}{2}\gamma^2)\, I_0(y\gamma)\,\gamma\,\mathrm{d}\gamma, \tag{18}$$

where I_0 is the modified Bessel function of the first kind of order zero. In particular, for homogeneous incompressible flows, we have the mean square velocity fluctuations being independent of the actual sampling (Eulerian/Lagrangian), i.e. $\langle u^2\rangle = \langle v^2\rangle$. The expression for the two-time, two-point correlation function $R_{\mathrm{E}}(\boldsymbol{\zeta}, \tau) = \langle \boldsymbol{v}(\boldsymbol{r}, t)\cdot \boldsymbol{v}(\boldsymbol{\zeta}+\boldsymbol{r}, t+\tau)\rangle$ can be obtained from (17) simply by replacing v_0 by ζ/τ. It can be shown that $R_{\mathrm{E}}(0, \tau)$ has a simple relation to $R_{\mathrm{L}}(\tau)$ in (12). In this limit the two functions become identical, apart from a factor $\sqrt{2}$ in the argument, see the Appendix and Wandel & Kofoed-Hansen (1962), or Pécseli & Mikkelsen (1986).

The normalized wavenumber spectrum $\mathscr{E}(k)$ entering (12) and (17) is given by the Fourier transform of the spatial correlation function $\langle \boldsymbol{v}(\boldsymbol{r},t)\cdot\boldsymbol{v}(\boldsymbol{r}+\boldsymbol{\zeta},t)\rangle/\langle u^2\rangle = R_{11}(\zeta)+R_{22}(\zeta)$, i.e. the sum of the longitudinal and lateral correlation functions. The spatial correlation tensor $\langle v_i(\boldsymbol{r})\,v_j(\boldsymbol{r}+\boldsymbol{\zeta})\rangle$ has the general form

$$R_{ij}(\boldsymbol{\zeta}) = g(\zeta)\,\delta_{ij}+[f(\zeta)-g(\zeta)]\frac{\zeta_i\,\zeta_j}{\zeta^2}. \tag{19}$$

With the stream function introduced before, these correlation functions can be given a simpler form with

$$f = -(1/\zeta)\,\mathrm{d}_\zeta R_\Phi(\zeta)/R''_\Phi, \quad g = -\mathrm{d}^2_\zeta R_\Phi(\zeta)/R''_\Phi = \mathrm{d}_\zeta(\zeta f), \tag{20}$$

where $R_\Phi(\zeta)$ is the scalar spatial correlation function for the stream function, where $R_\Phi(\zeta\to\infty)\to 0$ by choice of reference level and $R''_\Phi \equiv -\mathrm{d}^2_\zeta R_\Phi(\zeta=0)$. The notation $\mathrm{d}R_\Phi(\zeta)/\mathrm{d}\zeta \equiv \mathrm{d}_\zeta R_\Phi(\zeta)$ is used. Note that homogeneous and isotropic two-dimensional turbulence does not possess any lateral integral scale, i.e. $L_g \equiv \int g(\zeta)\,\mathrm{d}\zeta = 0$. The longitudinal lengthscale $L_f \equiv \int f(\zeta)\,\mathrm{d}\zeta$ is non-vanishing. The properties of the correlation tensor (19) and the spectral tensor for a two-dimensional system is discussed for instance by Pécseli & Mikkelsen (1985). Fourier transformation of the correlation function gives $\mathscr{E}(k) = (1/\pi)\int_0^\infty [f(\zeta)+g(\zeta)]\cos(k\zeta)\,\mathrm{d}\zeta$, by use of (19), see also Batchelor (1953).

The wavenumber spectrum can, however, be calculated from first principles when the form of the individual structures in (5) and (6) and their densities are known. It is most convenient to work with the stream function $\Phi = \sum_l \phi_l(\boldsymbol{r}-\boldsymbol{r}_l)$ according to (5). The correlation function R_Φ is by standard methods (Rice 1944) obtained as

$$\begin{aligned} R_\Phi(\zeta) &\equiv \langle \Phi(\boldsymbol{r})\,\Phi(\boldsymbol{r}+\boldsymbol{\zeta})\rangle \\ &= \sum_l \mu_l \int \phi_l(\boldsymbol{r})\,\phi_l(\boldsymbol{r}+\boldsymbol{\zeta})\,\mathrm{d}\boldsymbol{r}, \end{aligned} \tag{21}$$

where it is assumed that the structures are uniformly distributed in space with statistically independent positions. The summation in (21) runs over all structure shapes with individual densities μ_l. A possible d.c.-contribution in (21) is assumed to vanish by symmetry arguments, i.e. positive and negative amplitudes of a structure are assumed to be equally probable. Note that $R_\Phi(0) \neq 1$.

The present model allows the generation of a random flow which according to (21) can reproduce an arbitrary, prescribed, spatial correlation function, and therefore an arbitrary wavenumber spectrum. This is possible even with the use of only one type of randomly distributed structures. Given R_Φ in (21) a spatial structure for ϕ_l can be prescribed in indefinitely many ways since the convolution implied in (21) is insensitive to a phase factor. When only one type of structure is present (with both signs being equally probable) the problem is fully specified if both the correlation function and the triple correlation function are specified. In particular we have $\langle u^2\rangle \equiv 2u'^2 = 2R''_\Phi$ from (20) and (21). Evidently, the model implicitly assumes a complete randomness of the flow. Consequently, it is not applicable to organizing flows, for instance.

2.2. *Simplified derivation*

It is evident that the analysis summarized in the present section cannot accommodate arbitrary spatial variations for the structures defined by $\phi_l(\boldsymbol{r})$ in (21). Although the line-vortex model can be described by (5) and (6), the introduction of the corresponding logarithmic stream function in (21) will give rise to a divergence of the integral. It is worth pointing out that the main results summarized in §2.1 can be

obtained by quite different arguments, which may be helpful in providing an insight into the physical implications of the approximations made by Wandel & Kofoed-Hansen (1962) in their analysis. For this purpose consider first a frozen flow, where the wavenumber spectrum is known by a Fourier transform of (21). Let this flow realization move with constant velocity $\boldsymbol{u}$. A stationary observer will obtain a time-varying signal with an Eulerian correlation function given by

$$R_{\mathrm{E}}(\tau \mid u) = \int_0^\infty \mathscr{E}(k) \cos(ku\tau)\, \mathrm{d}k. \tag{22}$$

Now let $\boldsymbol{u}$ be randomly varying over the realizations of the ensemble. Assuming a Gaussian distribution for the components of $\boldsymbol{u}$ we have the probability density $(u/u'^2)\exp(-\frac{1}{2}(u/u')^2)$ for its magnitude, giving

$$R_{\mathrm{E}}(\tau) = \int_0^\infty \mathscr{E}(k) \int_0^\infty \gamma \cos(ku'\tau\gamma) \exp(-\tfrac{1}{2}\gamma^2)\, \mathrm{d}\gamma\, \mathrm{d}k, \tag{23}$$

reproducing (17) with $v_0 = 0$. Also the result for $v_0 \neq 0$ can be reproduced with a little more algebra, along the lines indicated here. It thus seems that the essentials of the analysis resulting in (17) amounts to assuming that structures are swept rapidly past an observer in such a way that the flow velocity convecting individual structures in each realization can be considered constant in the time interval it takes a structure to propagate its own diameter. The Gaussian distribution for the velocity can be argued as already discussed.

Also the expression (12) for the Lagrangian correlation function can be argued in a similar way. Consider a test particle being transported by the flow with a velocity $\boldsymbol{v}$, which will be considered essentially constant in a finite time interval. The flow generating $\boldsymbol{v}$ at the particle position is composed of a large number of overlapping structures. Out of all these structures those having velocities in a narrow interval around $\boldsymbol{u}$ are selected. The number of overlapping structures is assumed to be so large that the selected group will have a contribution to the spectrum $\mathscr{E}(k)$ which is independent of $\boldsymbol{u}$. This requirement is trivially satisfied if all the eddies are identical. Their contribution to the time-varying correlation function experienced by the test particle will of course depend on the selected velocity $\boldsymbol{u}$ as

$$R_{\mathrm{L}}(\tau \mid \boldsymbol{v}, \boldsymbol{u}) = \int_0^\infty \mathscr{E}(k) \cos(k\tau|\boldsymbol{u}-\boldsymbol{v}|)\, \mathrm{d}k. \tag{24}$$

Again $\boldsymbol{v}$ and $\boldsymbol{u}$ will be varying over all realizations having the same Gaussian probability density with standard deviation u'. (An interesting special case can be argued, where the probability densities of $\boldsymbol{v}$ and $\boldsymbol{u}$ are different. See Wandel & Kofoed-Hansen 1962.) However, the probability density for $|\boldsymbol{u}-\boldsymbol{v}|$ is then also a Gaussian with standard deviation $u'\sqrt{2}$. Salu & Montgomery (1977) use a somewhat similar argument in their discussion of Corrsin's hypothesis (Corrsin 1960). As one consequence we find that R_{L} is trivially related to $R_{\mathrm{E}}(0,\tau)$ as discussed in the Appendix. Another confirmation of this result can be obtained by (17) and noting that the foregoing arguments simply state that v_0 should be considered as a random variable with probability density $(v_0/u'^2)\exp(-\frac{1}{2}(v_0/u')^2)$. Carrying out the averaging over v_0 using $\int_0^\infty x\exp(-x^2) I_0(\beta x)\, \mathrm{d}x = \frac{1}{2}\exp(\frac{1}{4}\beta^2)$ again the same result is obtained. It is worth noting that the present summary reproduces the main results of Wandel & Kofoed-Hansen (1962) irrespective of a use of the series expansion implicit in (9).

A particular consequence of the simple relation between $R_{\mathrm{L}}(\tau)$ and $R_{\mathrm{E}}(\tau)$ in the present analysis is the corresponding relation between Lagrangian and Eulerian

integral timescales, i.e. $\tau_E = \tau_L\sqrt{2}$. The literature seems somewhat ambiguous concerning the relation between these two quantities. On one hand Lumley & Panofsky (1964) argued that $\tau_E < \tau_L$ since the Eulerian measurement correlates at every instant new fluid at the observation point, whereas the Lagrangian correlation deals always with the same fluid. Velocities are supposed to be more persistent along the path of a fluid particle than at a fixed observation point. Alternatively, Kraichnan (1964) argued that the frozen random flow presents a limiting case where obviously τ_E is infinite, while he expected τ_L to be finite. Also Leslie (1973) argued for $\tau_E > \tau_L$, by noting that measurements in a fixed position are sensitive to the long period (i.e. large-scale) disturbances. The Lagrangian correlation is swept around by these disturbances and should, therefore, be much less affected by them. It is interesting that the present model analysis supports the arguments for $\tau_E > \tau_L$. The ratio between Eulerian and Lagrangian micro timescales is $\tau_{mE}/\tau_{mL} = \sqrt{2}$ in the present model, i.e. the same as the ratio of the integral timescales. Tennekes (1975) has argued for $\tau_{mE}/\tau_{mL} \sim 1/Re^{\frac{1}{2}}$ in three-dimensional flows, where Re is the Reynolds number, i.e. $\tau_{mE} \ll \tau_{mL}$. The applicability of these results for moderate or small Re have been criticized, however, by Yeung & Pope (1989).

2.3. *Relation to Corrsin's hypothesis*

A potentially useful relation between Eulerian and Lagrangian correlation functions was argued by Corrsin (1960) on intuitive grounds. The justification of this hypothesis was discussed by, for instance, Weinstock (1976) while Peskin (1974) performed a numerical simulation for investigating its range of validity. We found it worthwhile to compare our results with those conjectured by Corrsin (1960), which, for the correlation tensors with elements denoted by the subscript ij, can be formulated as

$$R_L(\tau)_{ij} = \int_{-\infty}^{\infty}\int_{-\infty}^{\infty} R_E(r,\tau)_{ij}\, P(r,\tau)\,\mathrm{d}\boldsymbol{r}, \tag{25}$$

where $P(r,\tau)$ is the probability density for particle displacement for a particle which is known with certainty to be at $r = 0$ at $\tau = 0$, i.e. $P(r,\tau=0) = \delta(r)$. In particular, (25) gives in our notation for R_L in (9) and R_E in (17)

$$R_L(\tau) = 2\pi\int_0^{\infty} R_E(r,\tau)\, rP(r,\tau)\,\mathrm{d}r. \tag{26}$$

With a little algebra, which makes use of the results in the Appendix, it is readily demonstrated that our results (12) and (17) satisfy (26), provided we take $P(r,\tau) = (1/2\pi)(u't)^{-2}\exp(-\frac{1}{2}(r/u't)^2)$. This form is, however, not consistent with that postulated for P in (25). This is readily seen by considering $\langle r^2\rangle$ obtained for a particle released at the origin for $t = 0$, which is given by

$$\langle \boldsymbol{r}^2\rangle = 2t\langle u^2\rangle\int_0^t (1-\tau/t)\, R_L(\tau)\,\mathrm{d}\tau, \tag{27}$$

for homogeneous isotropic turbulence, see e.g. Lumley & Panofsky (1964). For small times (27) gives $\langle r^2\rangle \approx \langle u^2\rangle t^2$ which is consistent with $\langle r^2\rangle = \int_{-\infty}^{\infty} r^2 P(r,t)\,\mathrm{d}\boldsymbol{r}$. For large times, however, in the diffusion limit, the result is $\langle r^2\rangle \approx \langle u^2\rangle t\int_0^{\infty} R_L(\tau)\,\mathrm{d}\tau$ which is not consistent with our expression for $P(r,t)$. Although our analytical result for R_L resembles the one obtained by Corrsin's hypothesis, the two expressions are not identical. The derivations are, after all, also fundamentally different. It is interesting, though, that (25) will imply in general (Weinstock 1976) that

$R_L(\tau) \leqslant R_E(\tau)$ in agreement with our results. Corrsin's analysis does not contain any analogue to our relation (17).

3. Numerical results

A numerical code was developed in order to simulate a system containing a large number of structures which evolve according to (3)–(4), written in normalized units. The code is in principle quite straightforward and need not be described in particular detail. The calculations are carried out in double precision and the displacement in the coordinates of the individual structures are followed. This is a rather time-consuming procedure which, for computational reasons, restricts the number of structures to at most a few thousand. Typically, in the simulations described in the following sections, we used 1800 interacting structures, with imposed symmetry conditions to be described. A significant increase in the number of structures would require interpolation in a grid representation of the flow. The resulting numerical inaccuracy could give rise to a randomness in the structure trajectory which would be in disagreement with the one assumed in the model. Our calculations are carried out in a large square system with sidelength $3L$, with the requirement that the number of structures in each of the 9 cells with area L^2 is the same. A symmetry requirement is imposed by generating 8 positions from all positions of structures in the central cell, i.e. a position (x_l, y_l) gives rise also to $(x_l \pm L, y_l)$, $(x_l, y_l \pm L)$ and $(x_l \pm L, y_l \pm L)$. This procedure ensures that the number of structures in each of the 9 cells is constant, i.e. if a structure leaves a cell another one enters simultaneously at the opposite position in the same cell. The procedure outlined here is effectively tantamount to imposing periodic boundary conditions provided L is much larger than the spatial extent of any structure in the system. The timestepping is accomplished by a partially corrected third-order Adams–Bashforth scheme, see Gazdag (1976), except for the first step, which is a simple Euler step, and the second one which is a leap-frog step. For Hamiltonian systems the conservation of H in (7) is used as a test for the accuracy of the code, for a given timestep. Simple cases with only two structures in the central cell are used for additional tests. Here the solution is known exactly. For the simulations discussed in the following the initial positions of the structures were generated by standard random number generators on the computer. Test runs (not discussed here) were carried out for other initializations.

Spatial correlations are obtained by recording time series for velocity components in selected points along the diagonal of a subcell with side length $\frac{1}{2}L$. The correlation length of the fluctuating fields as obtained from (17) are smaller than $\frac{1}{2}L$ in all cases investigated. Likewise the correlation time is smaller than the time it takes, on average, for a vortex to traverse the distance $\frac{1}{2}L$. The periodicity of our system can be ignored, and the subcell considered as representative for an element of an extended, homogeneous and isotropic flow. Lagrangian correlations are obtained both by following test particles in the flow, and for selfconsistently moving structures.

The analysis summarized in §2 is in principle applicable for any shape of the structures (provided the integral exists) but the resulting expressions will in general have to be solved numerically. In the present study we consider only the case where the individual structures are described by

$$\phi_l = A_l \exp(-r^2/\delta_l), \tag{28}$$

characterized by only two parameters A_l and δ_l. With this simple form all our

(a)

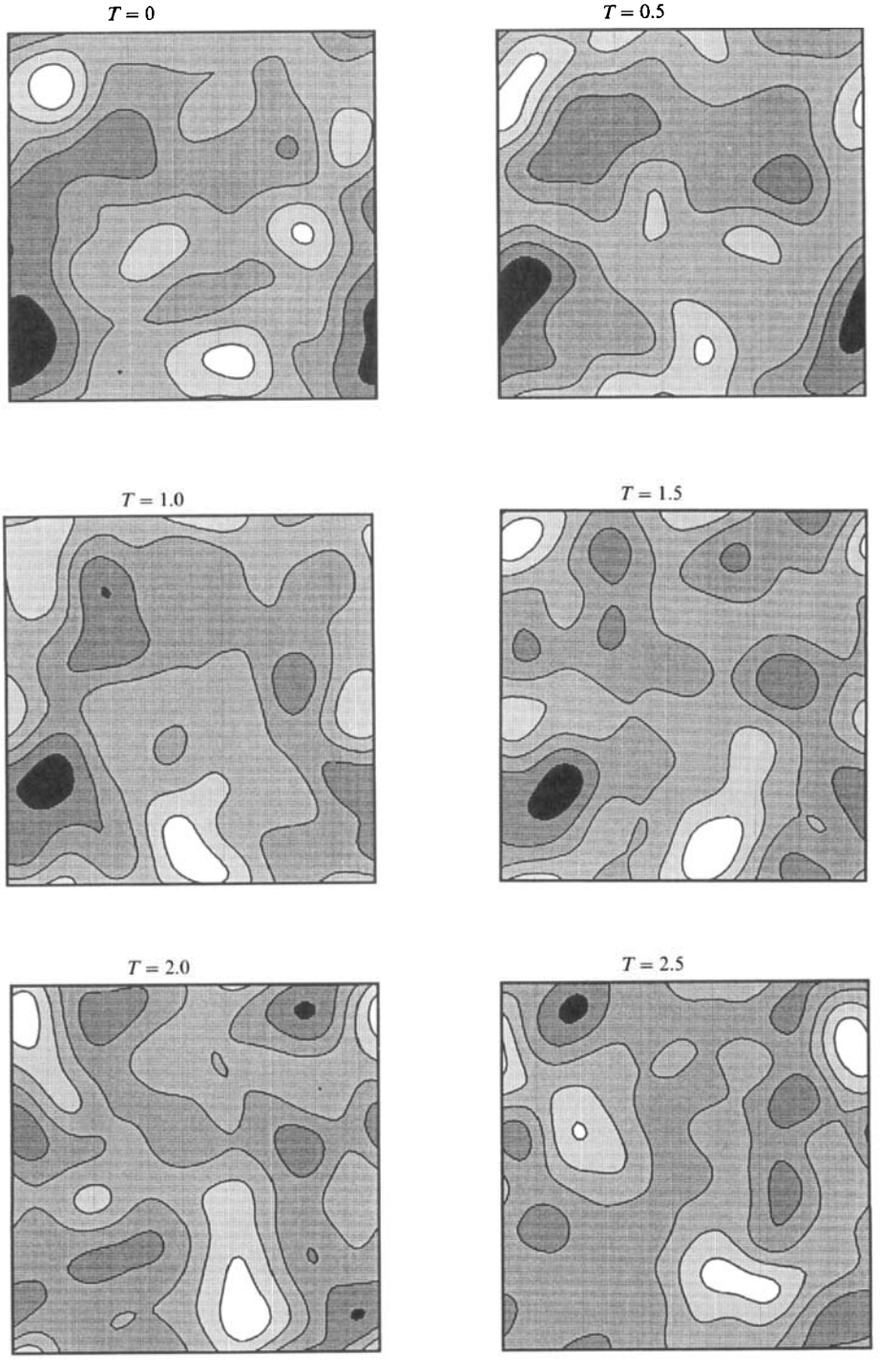

FIGURE 1 (a). For caption see facing page.

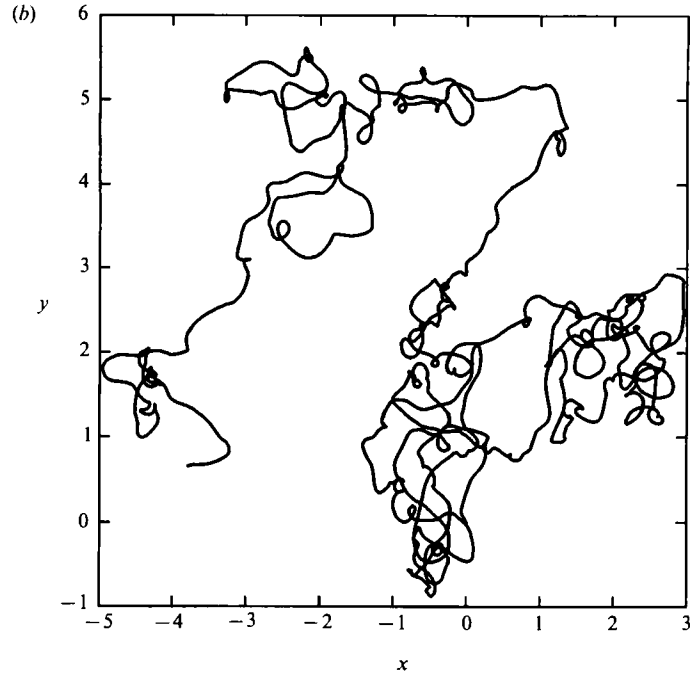

FIGURE 1. (*a*) Time sequence showing the evolution of the streamfunction for 200 structures of each polarity with $|A_l| = 1$ and $\delta_l = \frac{1}{2}$. Note that individual structures cannot be discriminated by visual inspection. Black regions are negative while white regions are positive. The full system is periodic, as explained in the text. (*b*) Trajectory of one typical vortex, initially at $(x, y) = (0, 0)$.

expressions from §2 can be solved analytically. Two cases are considered: one where δ_l is the same for all structures and only A_l is varying with l. This system was shown to be Hamiltonian in §1. As an illustration we give a time sequence for the evolution of the stream function in figure 1 together with the trajectory of a typical vortex. In the other case studied, also δ_l is allowed to vary.

In all cases considered we had $\delta \ll L$. The periodicity imposed on the distribution of structures, which is a convenient computational simplification, is therefore immaterial for the interpretation of the numerical results. The computations were rather time consuming, and for practical reasons the density of structures could not be made arbitrarily large. Because many of the structures which compose the flow are overlapping, they are not individually discernible in a realization as in figure 1. We note, however, that incidental groups or clusters of structures (see e.g. the white or black regions in figure 1) will be deformed and distorted by the flow as discussed in §1.

3.1. *Structures with same widths and amplitudes*

First we consider the case where $\delta_l = \delta$ and $|A_l| = A$ for all l with an equal number of structures of the two polarities. The most important parameter for the problem is the density of structures $\mu = N/L^2$ where N is the number of structures in a cell. A central assumption in the analysis summarized in §2 was that the velocity components have a Gaussian probability density, which follows from the assumption that many eddies contribute to the velocity at a selected point. The number of overlapping eddies is on average of the order $4\delta\mu$. It is well known, however, that this quantity need not be particularly large, i.e. a number larger than 4–5 will suffice for producing a probability density which is in practice indiscernible from a Gaussian.

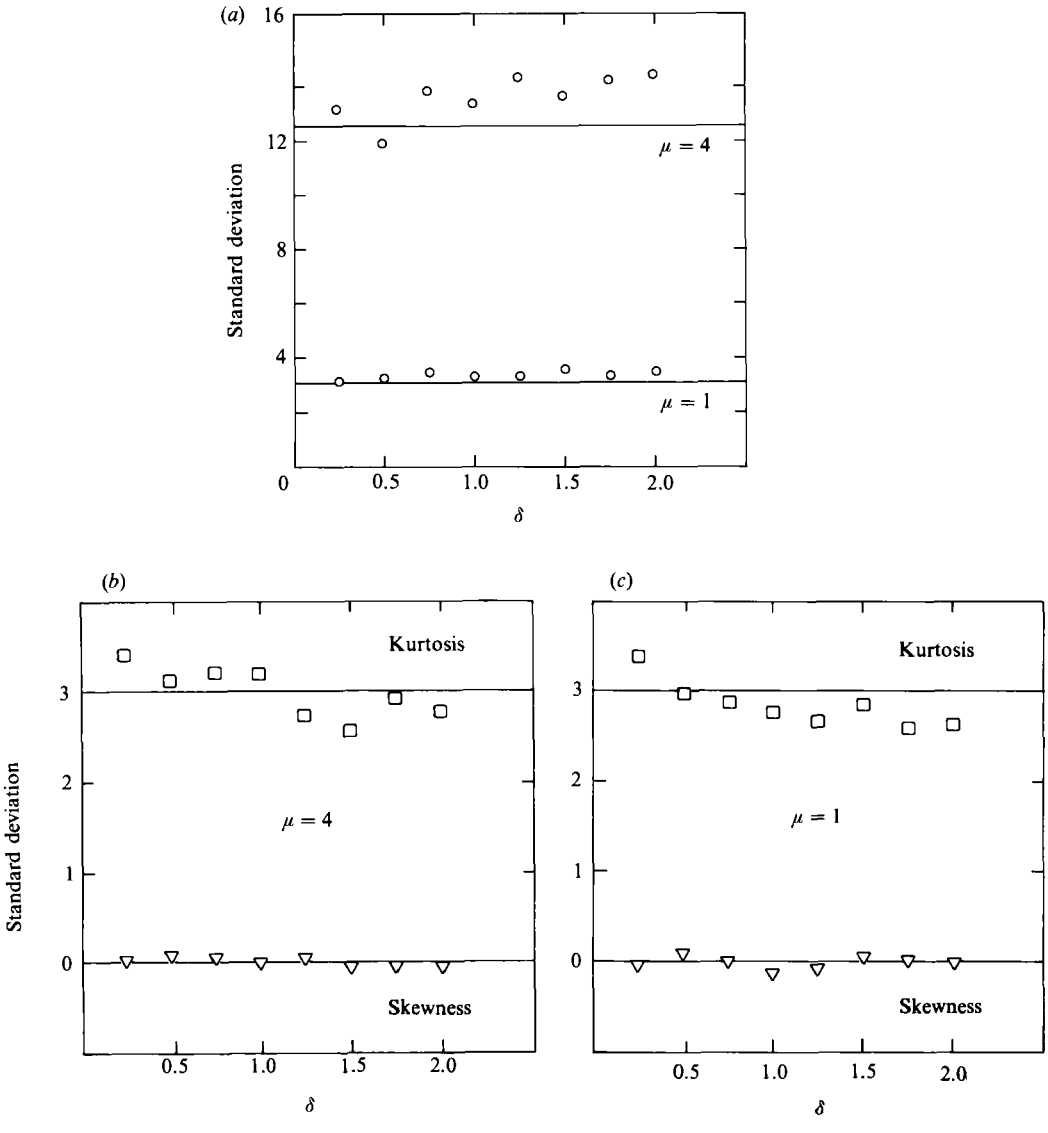

FIGURE 2. Variation of standard deviation (○), skewness (△), and kurtosis (□), for varying width, δ, of the structures. Two different densities $\mu = 1$ and $\mu = 4$, were considered. Solid lines are the results expected for Maxwellian distributions.

We characterize the probability density for the velocity components by its lowest-order moments, i.e. standard deviation, skewness and kurtosis. In figure 2 we show the variation of these three quantities for varying δ and two values of μ. The results are obtained as an average over an interval of 24 time units (i.e. 2400 timesteps). For reference we give, by full lines, the variations according to our model.

The value for $\langle u^2 \rangle$ used in figure 2 was determined by first calculating the stream function correlation function obtained from (21)

$$R_\Phi(\zeta) = \tfrac{1}{2}\pi \frac{NA^2}{L^2} \delta \exp\left(-\zeta^2/(2\delta)\right), \tag{29}$$

giving $R''_\Phi = (\tfrac{1}{2}\pi)(NA^2/L^2)$, i.e. $\langle u^2 \rangle = \pi\mu A^2$, while $\langle \Phi^2 \rangle = \tfrac{1}{2}\pi\mu A^2\delta$.

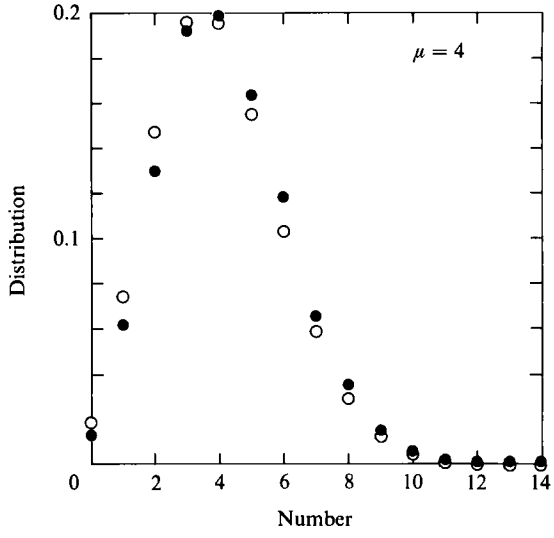

FIGURE 3. Distribution of the numbers of structure centres in a small area element $\Delta = 1$ for $\mu = 4$ obtained from the simulation with $\delta = \frac{1}{2}$ and $|A| = 1$. Open circles show the results from a Poisson distribution with the corresponding parameters.

Implicit in the derivation of Wandel & Kofoed-Hansen (1962) is the assumption that the distribution of eddies (or, more correctly, structure centres) in a volume element follows a Poisson distribution, i.e. in the present case the number, k, of structure centres in an area element Δ is distributed according to $P(k) = (\Delta\mu)^k \exp(-\Delta\mu)/k!$ If two area elements are non-overlapping then the two corresponding Poisson distributed random variables are independent. Since the equations of motion (3)–(4) certainly introduces a correlation between all the structures, the assumption of a Poisson distribution cannot be exact. In the limit of small μ, all structures are essentially isolated and they are consequently not convected at all. For low structure densities, convection will be induced primarily when two structures of opposite polarity happen to overlap, and they will propagate along an orbit characterized by their bulk properties. The orbit is a straight line if the structures are identical apart from a sign of amplitude. Two structures of the same polarity will rotate around a suitably defined centre of mass. In either case structures will appear in pairs. However, again in the limit of large densities it might be expected that the correlation between individual structures is small. The assumption of a Poisson distribution mentioned before may then be appropriate. In figure 3 we show, with filled circles, the distribution of structure centres in a normalized area element 1 for $\mu = 4$. Open circles show the results for a Poisson distribution for the given parameters. We find the agreement quite acceptable.

Using (20) with (29) we readily obtain the expressions for the longitudinal and lateral correlation functions as

$$f(\zeta) = \exp(-\zeta^2/(2\delta)), \tag{30}$$

and

$$g(\zeta) = (1/\delta)(\delta - \zeta^2)\exp(-\zeta^2/(2\delta)). \tag{31}$$

The numerical results are shown in figure 4 with the analytical results (30) and (31) given by a dotted line. The agreement seems fully satisfactory. In particular we confirmed that $R_{12}(\zeta) = 0$ within the statistical uncertainty, see (19). In figure 4(*c*) the flatness factor is shown for both longitudinal and transverse velocity components.

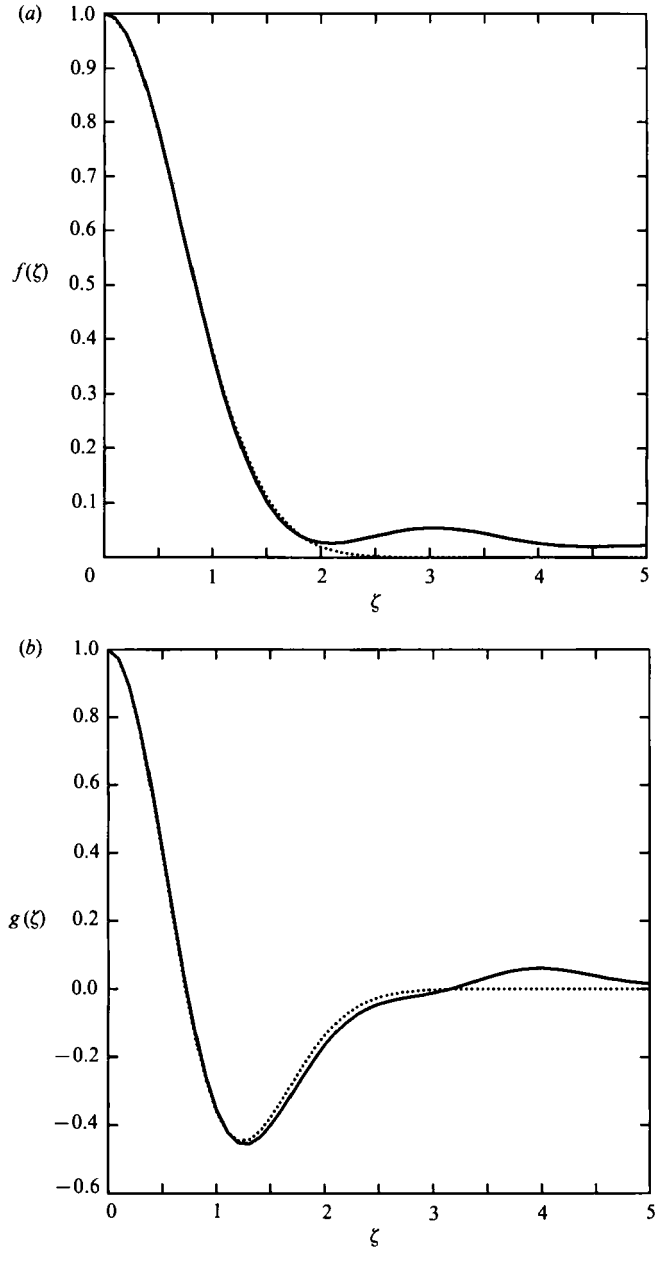

FIGURE 4 (a, b). For caption see facing page.

These results indicate that the joint probability density of the fluctuating velocity is close to a bivariate Gaussian, where the flatness factor is 3 for all separations. This result is expected for a random superposition of many structures (Rice 1944). For the particularly simple model (28) used here, it is possible to solve (17)–(18) analytically with the result

$$R_{\mathrm{E}}(\zeta,\tau)=\frac{1+(\tau u')^2/\delta-\frac{1}{2}\zeta^2/\delta}{(1+(\tau u')^2/\delta)^3}\exp\left(-\tfrac{1}{2}(\zeta^2/\delta)/(1+(\tau u')^2/\delta)\right), \tag{32}$$

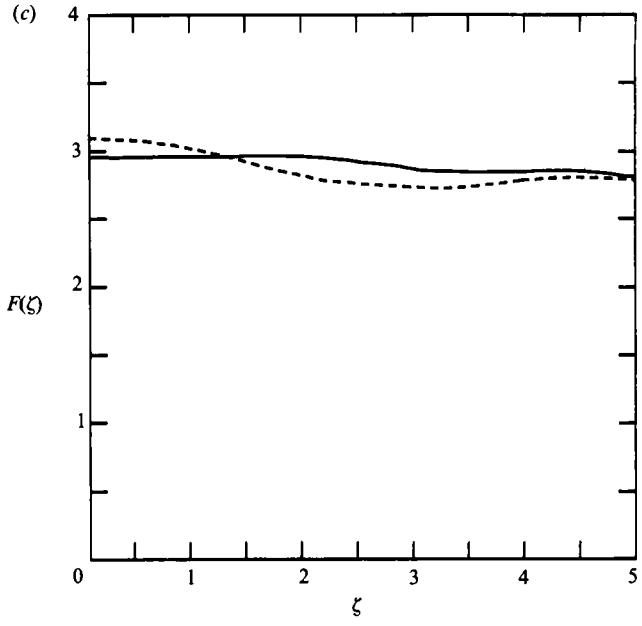

FIGURE 4. Results from the numerical simulation for (*a*) the longitudinal and (*b*) the lateral correlation functions, respectively. The dotted line gives the analytical results from (30) and (31). The averages are obtained from a simulation with a normalized timespan of 120 with timestep 10^{-2}. The parameters are $|A| = 1$, $\delta = \frac{1}{2}$ and $\mu = 4$. (*c*) Flatness factor $F(\zeta) = \langle [v_i(r_1+\zeta, r_2) - v_i(r_1, r_2)]^4 \rangle / \langle [v_i(r_1+\zeta, r_2) - v_i(r_1, r_2)]^2 \rangle^2$ for longitudinal (full line) and transverse (dashed line) velocity components.

where we used $\mathscr{E}(k) = (\delta/2\pi)^{\frac{1}{2}}(1+k^2\delta)\exp(-\frac{1}{2}\delta k^2)$ in (17). Figure 5 shows (32) for varying τ and ζ. In the limit $\zeta = 0$ the relation

$$R_{\mathrm{E}}(0,\tau) = \frac{1}{(1+(\tau u')^2/\delta)^2} \tag{33}$$

is obtained, while $\tau = 0$ gives $R_{\mathrm{E}}(\zeta, 0) = (1-\frac{1}{2}\zeta^2/\delta)\exp(-\frac{1}{2}(\zeta^2/\delta))$ which reproduces $R_{\mathrm{E}}(\zeta, 0) = \frac{1}{2}[f(\zeta)+g(\zeta)]$ as it should. The limit $\tau \to 0$ is thus already analysed by figure 4, where, as already mentioned, the expression (32) is in excellent agreement with our numerical results. For $\tau \neq 0$ we found that the largest disagreement is obtained for $R_{\mathrm{E}}(0,\tau)$, i.e. the limit given by (33). These results are shown in figure 6 with (33) represented by a dotted curve. Close to the origin the agreement between the two curves is actually quite good, but the disagreement for large τ is obviously an indicator of a shortcoming in the model. An increase of ζ results in successively improving agreement between the numerical and analytical results. Finally the Lagrangian correlation function is determined as (see the Appendix)

$$R_{\mathrm{L}}(\tau) = \frac{1}{(1+2(\tau u')^2/\delta)^2}. \tag{34}$$

Figure 7 shows numerical results where (34) is included by a dotted curve for comparison. In this case the agreement is quite good. At first sight it seems paradoxical that (34) gives such a good representation for the numerically simulated dynamics, while the seemingly similar expression (33) is giving only a modest approximation to the Eulerian correlations. It should however be noted, having in

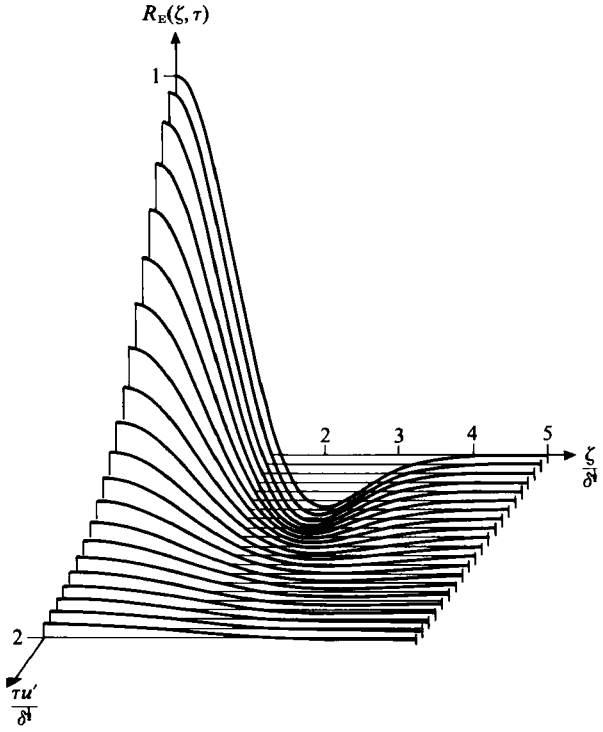

FIGURE 5. The analytical expression for the Eulerian correlation function $R_E(\zeta,\tau)$, shown as a function of ζ for different τ. Parameters are as in figure 4.

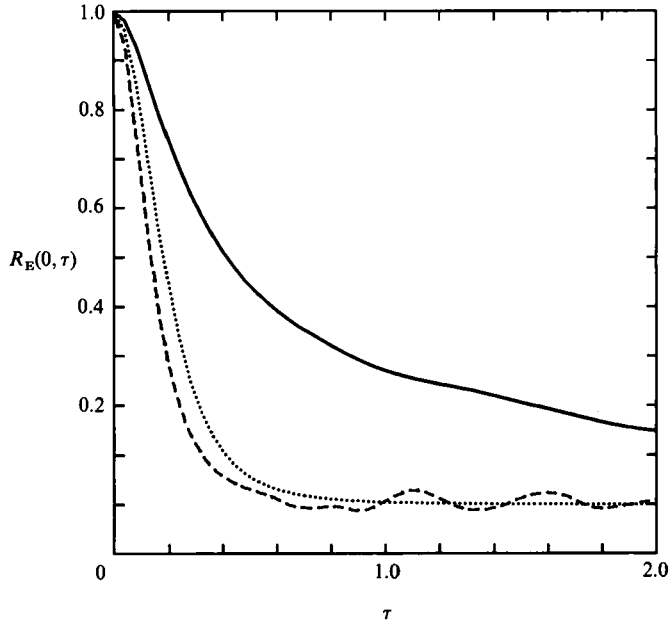

FIGURE 6. Numerical results for $R_E(0,\tau)$ with the analytical expression represented by a dotted line. The dashed line shows numerical results where the individual structures are moving along straight line orbits with constant velocities which are chosen randomly from a Gaussian distribution. Parameters are as in figure 4.

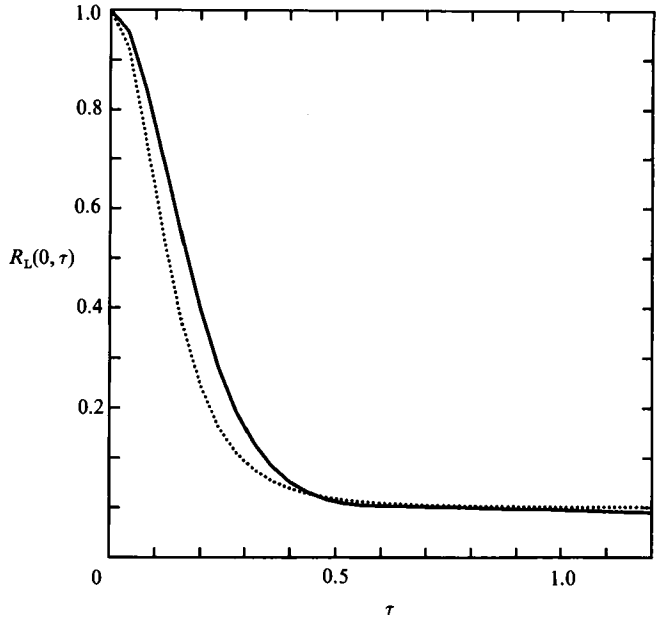

FIGURE 7. Numerical results for the Lagrangian velocity correlation function $R_L(\tau)$ with the analytical expression represented by a dotted line. Parameters are as in figure 4.

mind the simple physical discussion in §2.2, that the analytical results implicitly assume that eddies are swept rapidly past the observation point. This assumption is evidently best satisfied when the observation point is itself moving as, for example, in Lagrangian sampling. With the substitution $r_0 = v_0 t$ in (32) corresponding to Eulerian sampling in a moving frame, as in (17), we again obtained a good agreement between numerical and analytical correlation functions, as already mentioned. Our numerical results for the Eulerian correlation function provide evidence in favour of Leslie's (1973) physical argument quoted previously, i.e. the Eulerian correlation function seems particularly sensitive to large-scale fluctuations.

Ignoring (6) and prescribing straight-line trajectories for the structures with a Gaussian distribution of velocities we obtain a very good agreement with (33). These results are shown by a dashed line in figure 6. The deviations from (33) observed in figure 6 thus originate from time variations in the velocities during a structure transit time which will be particularly conspicuous for variations in slow structure velocities.

Calculations as those summarized in this section have been repeated with parameters $|A| = 1$, $\delta = \frac{1}{2}$ and $\mu = 8$. The result agree with those from the simulations with $\mu = 4$, within the statistical uncertainty.

Intuitively it could be expected that an increase in $\langle u^2 \rangle$ would give rise to better agreement between numerical and analytical results for the Eulerian correlation functions. However, attempts to increase $\langle u^2 \rangle$ inevitably brings the system into the negative temperature regime characterized by a long-range ordering, and the basic assumptions in the analysis of §2 are invalidated. In our simulations the transition becomes apparent by an increase in correlation lengths as compared to those obtained, for example, from figure 4. The transition comes rather gradually and the value for the energy where the temperature changes sign is poorly defined by these numerical results.

3.2. *Structures with statistically distributed amplitudes*

A simple generalization of the results of §3.1 is obtained by retaining the form (28) with δ_l = constant, but let A_l be a quantity which varies randomly with l. When all A_l have the same distribution the results of §3.1 are readily generalized by the extension of Campbell's theorem given by Rice (1944) and for instance (29) is trivially generalized by use of (21). The important point here is that the Hamiltonian (7) applies for the present problem also. The numerical simulations were extended to cover also the case where A_l varied. In order to ensure that $\int \phi \, \mathrm{d}r = 0$ we included structures pairwise with both polarities of A_l for varying l. We considered a case with an equal number of amplitudes 1.2 and 0.8 and $\delta = 0.5$. Another simulation used a random number generator with amplitudes distributed in the range [0.8; 1.2] so that the average remained 1.0 also with $\delta = 0.5$. Finally we considered the case with amplitudes $A_i = 0.5$, 1.0, 1.5 and 2.0 all with same density $\mu_i = 1$ while $\delta = 1$. Comparing the numerically obtained correlation functions with the analytical results we found the same overall agreement as the one found in §3.1, maybe with a slight improvement, which however was within the statistical uncertainty. In particular we did not find any noticeable improvement in the agreement with the analytical expression for the Eulerian correlation function.

3.3. *Structures with distributed amplitudes and widths*

Our numerical simulations were generalized also to the case where the amplitudes as well the widths of the structures given by (28) were distributed. This case is principally different from those discussed in §§3.1 and 3.2 since (7) is no longer conserved. The analytical expressions (12) and (17) for the correlation functions are derived independently of a Hamiltonian formalism and can easily be generalized. For example the Lagrangian correlation function becomes

$$R_{\mathrm{L}}(\tau) = \frac{1}{\langle u^2 \rangle} \sum_{l}^{M} \frac{\pi \mu_l A_l^2}{(1 + \tau^2 \langle u^2 \rangle / \delta_l)^2}, \tag{35}$$

with

$$\langle u^2 \rangle = \pi \sum_{l}^{M} \mu_l A_l^2, \tag{36}$$

where (28) was explicitly used in (12). The number of possible different structures, characterized by A_l and δ_l, which can appear in each realization is denoted by M in (35), and their density is μ_l. The number M is thus not a quantity referring to an actual realization.

The numerical simulations were carried out for a number of different cases: (i) amplitudes $A = 1$ and widths $\delta = 0.3$ and $\delta = 0.9$, (ii) $A = 1$ with $\delta = 0.3$ and $\delta = 0.8$ and (iii) the combination $A = 0.8$, $\delta = 0.3$ and $A = 1.2$, $\delta = 0.8$ in equal numbers, each with densities $\mu = 2$. The overall agreements between the theoretical and the numerically obtained correlation functions was quite similar to those summarized in the foregoing sections. To be more specific we introduced a measure e for the difference between the numerical and theoretical results as

$$e = \frac{\left[\int_0^\infty [R_{\mathrm{L,T}}(\tau) - R_{\mathrm{L,N}}(\tau)]^2 \, \mathrm{d}\tau \right]^{\frac{1}{2}}}{\left[\int_0^\infty R_{\mathrm{L,T}}(\tau) R_{\mathrm{L,N}}(\tau) \, \mathrm{d}\tau \right]^{\frac{1}{2}}}, \tag{37}$$

shown here in terms of the Lagrangian correlation function, where $R_{L,N}$ is its numerical obtained value while $R_{L,T}$ is the theoretical expression. Limiting the integrations in (37) to the interval $[0;1.5]$ we obtain $e = 0.24 \pm 0.06$ for the Lagrangian correlation function, noting that the integral timescale defined by $R_{L,N}(\tau)$ was consistently larger than the one obtained by $R_{L,T}(\tau)$.

4. Conclusions and discussions

The relation between Eulerian and Lagrangian correlation functions has been studied in to a two-dimensional autonomous flow model, which can be considered as a generalization of Onsager's line-vortex model. The results from a numerical simulation, where the properties of the model were implemented, were compared with analytical expressions for the correlation functions obtained by applying the ideas of Wandel & Kofoed-Hansen (1962) in a two-dimensional representation. In agreement with the simulation model this analysis assumes that a randomly varying flow is represented by a superposition of coherent structures in the form of vortices where each one propagates without change in shape along a trajectory which is determined by the combined convective effect of all other structures. In the present analysis we used a particularly simple shape for the individual structures (28) characterized by only two parameters, i.e. an amplitude and a width. By use of this simple form all analytical results can be expressed in a closed form where the distribution of the parameters enter. The Eulerian correlation function $R_E(\zeta, \tau)$ as well as its Lagrangian counterpart $R_L(\tau)$ are expressed in terms of the same wavenumber spectrum integrated together with weight functions containing the amplitudes, widths and densities of the structures as parameters. The conclusions from a comparison between the numerical and analytical results can be summarized as follows: for the limiting case $R_E(\zeta, \tau = 0)$ we found a very good agreement in all cases investigated. As τ is increased the agreement becomes progressively worse where the limit $R_E(\zeta = 0, \tau)$ gives the most pronounced disagreement between theory and simulations, where in particular the Eulerian correlation time from the simulations exceeded the theoretical value (see figure 6). We observed, however, that, in the limit where the product $\delta\mu$ exceeded a value around 1 in the simulations the micro-timescale defined by $[\mathrm{d}_\tau^2 R_E(0,\tau)]_{\tau=0}^{-\frac{1}{2}}$ is in quite good agreement with its analytical expression. In the same limit a good agreement was found for the Lagrangian correlation function $R_L(\tau)$ for all values of τ, see e.g. figure 7. The latter results were independent of the conservation of the Hamiltonian (7) by the model. The limit $\delta\mu \geqslant 1$ implies that in any given point more than four structures contribute, on average, to the local bulk velocity obtained by the superposition (3) or (5). For computational reasons we considered only cases where $\mu \leqslant 8$. For a typical value of $\delta = \frac{1}{2}$ we found, however, that $\mu > 2$ was sufficient to ensure that the probability densities of the velocity components were close to Gaussians.

The diffusion of passive particles can readily be investigated in the simulations of the model. The mean square displacement of a particle with respect to its origin of release is given by e.g. Lumley & Panofsky (1964) by the expression (27). We have not carried out any particular study of the mean square displacement since the results can easily be derived from $R_L(\tau)$ which we have analysed in detail.

The basic result of our study was a demonstration that within the present model the Lagrangian correlation function, to quite good approximation, could be obtained from an expression (12) which involved as input parameters only the wavenumber power-spectrum $\mathscr{E}(k)$ and the mean-square fluctuation level $\langle u^2 \rangle$. The weight

function $W(\zeta)$ in (12) is an *a priori* given quantity. With both $\mathscr{E}(k)$ and $\langle u^2 \rangle$ being measurable quantities, the relation (12) and its three-dimensional analogue, can be postulated as universal approximations valid irrespective of the model from which they were derived. Actually Wandel & Kofoed-Hansen (1962) and Kofoed-Hansen & Wandel (1967) presented arguments for a rather general validity of the approximation and at least applied to the Hay–Pasquill (1960) hypothesis the results proved quite convincing. A study of the general applicability of (12) is in progress, using a two-dimensional flow simulation based on the Euler equations.

Finally, we should like to point out that simulations like the ones used in the present work can be useful for testing methods for recovery of large coherent structures in turbulent flows (see e.g. Hussain 1986). The flow in our simulation is composed entirely of coherent structures, and we find it worth noting that the lowest-order approximation advocated by Adrian (1979) and Adrian & Moin (1988) will produce signatures for double-vortex structures. As pointed out by Pécseli & Mikkelsen (1986) this result could be fundamentally misleading, since the flow is, by construction in our case, composed of monopole-type structures.

We thank O. Kofoed-Hansen and C. F. Wandel for valuable discussions in the initial stages of this study.

Appendix

In this Appendix we will prove the identity

$$R_{\mathrm{L}}(\tau/\sqrt{2}) = R_{\mathrm{E}}(0,\tau), \tag{A 1}$$

where R_{L} is given by (12) while $R_{\mathrm{E}}(0,\tau)$ is obtained from (17) with $v_0 = 0$. Following Pécseli & Mikkelsen (1985, 1986) we use the series expansions

$$W(x) = 1 + \sum_{n=0} (-1)^{n+1} \frac{x^{2n+2} 2^n n!}{(2n+1)!} \tag{A 2}$$

and

$$\cos x = \sum_{n=0} (-1)^n \frac{x^{2n}}{(2n)!}$$

giving,

$$\begin{aligned} \int_0^\infty \gamma \cos(x\gamma) \exp(-\tfrac{1}{2}\gamma^2)\, \mathrm{d}\gamma &= 1 + \sum_{n-1} (-1)^n \frac{x^{2n} 2^n n!}{(2n)!} \\ &= 1 + \sum_{n=0} (-1)^{n+1} \frac{x^{2n+2} 2^{n+1} (n+1)!}{(2n+2)!} \\ &= 1 + \sum_{n=0} (-1)^{n+1} \frac{x^{2n+2} 2^n n!}{(2n+1)!} \end{aligned} \tag{A 3}$$

by using the substitution $n \to n+1$. The relation (A 1) then follows by introducing the arguments of the functions in (12) and (17) since $u'^2 = \frac{1}{2}\langle u^2 \rangle$. The identity (A 2) = (A 3) demonstrates that $W(x)$ is simply the cosine transform of the Rayleigh distribution.

The result (A 1) implies $R_{\mathrm{L}} < R_{\mathrm{E}}$ for all times. It is interesting that the results of Weinstock (1976) and also Reeks (1977) support this inequality, at least for large τ, see also the three-dimensional flow simulations of Yeung & Pope (1989).

REFERENCES

ADRIAN, R. J. 1979 *Phys. Fluids* **22**, 2065.

ADRIAN, R. J. & MOIN, P. 1988 *J. Fluid Mech.* **190**, 531.

BATCHELOR, G. K. 1953 *The Theory of Homogeneous Turbulence*. Cambridge University Press.

CHORIN, A. J. 1973 *J. Fluid Mech.* **57**, 785.

CORRSIN, S. 1960 In *Atmospheric Diffusion and Air Pollution* (ed. F. N. Frenkiel & P. A. Sheppard), p. 162. (Advances in Geophysics, vol. 6) Academic.

EWALD, P. P. 1921 *Annln Phys.* (Leipzig) **64**, 253.

GAZDAG, J. 1976 *J. Comput. Phys.* **20**, 196.

HAY, J. S. & PASQUILL, F. 1960 Adv. Geophys. **6**, 345.

HINZE, J. O. 1975 *Turbulence*, 2nd edn. McGraw-Hill.

HULD, T., IIZUKA, S., PÉCSELI, H. L. & RASMUSSEN, J. J. 1988 *Plasma Phys. Contr. Fusion* **30**, 1297.

HUSSAIN, A. K. M. F. 1986 *J. Fluid Mech.* **173**, 303.

JOYCE, G. & MONTGOMERY, D. 1973 *J. Plasma Phys.* **10**, 107.

KNORR, G. & PÉCSELI, H. L. 1989 *J. Plasma Phys.* **41**, 157.

KOFOED-HANSEN, O. & WANDEL, C. F. 1967 *Risø Rep.* no. 50.

KRAICHNAN, R. H. 1964 *Phys. Fluids* **7**, 142.

LESLIE, D. C. 1973 *Developments in the Theory of Turbulence*. Clarendon Press.

LUMLEY, J. L. & PANOFSKY, H. A. 1964 *The Structure of Atmospheric Turbulence*. Interscience.

MONTGOMERY, D. & JOYCE, G. 1974 *Phys. Fluids* **17**, 1139.

ONSAGER, L. 1949 *Nouvo Cimento Suppl.* **6**, 279.

PANOFSKY, H. A. & DUTTON, J. A. 1984 *Atmospheric Turbulence*. John Wiley.

PÉCSELI, H. L. & MIKKELSEN, T. 1985 *J. Plasma Phys.* **34**, 77.

PÉCSELI, H. L. & MIKKELSEN, T. 1986 *Plasma Phys. Contr. Fusion* **28**, 1025.

PESKIN, R. L. 1974 In *Turbulent Diffusion in Environmental pollution* (ed. F. N. Frenkiel & R. E. Munn), p. 141. (Advances in Geophysics, vol. 18A) Academic.

REEKS, M. W. 1977 *J. Fluid Mech.* **83**, 529.

RICE, S. O. 1944 *Bell System Tech. J.* **23**, 282 and 1945, *Bell System Tech. J.* **24**, 46. Reprinted in *Selected Papers on Noise and Stochastic Processes* (ed. N. Wax) 1954, Dover.

SALU, Y. & MONTGOMERY, D. 1977 *Phys. Fluids* **20**, 1.

SEYLER, C. E., SALU, Y., MONTGOMERY, D. & KNORR, G. 1975 *Phys. Fluids* **18**, 803.

SULEM, C. & SULEM, P. L. 1983 *J. Méc. Numéro Special*, 217.

SULEM, C., SULEM, P. L. & FRISCH, H. 1983 *J. Comp. Phys.* **50**, 138.

TENNEKES, H. 1975 *J. Fluid Mech.* **67**, 561.

WANDEL, C. F. & KOFOED-HANSEN, O. 1962 *J. Geophys. Res.* **67**, 3089.

WEINSTOCK, J. 1976 *Phys. Fluids* **19**, 1702.

YEUNG, P. K. & POPE, S. B. 1989 *J. Fluid Mech.* **207**, 531.